Relaxation process during the selective oxidation of aqueous ethanol with oxygen on a platinum catalyst

Relaxation Processes during the Selective Oxidation of Aqueous Ethanol with Oxygen on a Platinum Catalyst

Ludo Jelemensky, Ben F. M. Kuster,* and Guy B. Marin

Laboratorium voor Chemische Technologie, Schuit Institute of Catalysis, Eindhoven University of Technology, P.O. Box 513, 5600 MB Eindhoven, The Netherlands

The observed loss of activity at constant conditions during the selective oxidation of ethanol with oxygen in a continuous stirred-tank reactor with carbon-supported platinum can be described by a model considering reversible transformations between three oxidizing species on the catalyst. One of these species is much more reactive toward ethanol and can be considered as a reaction intermediate in the selective oxidation of the latter. The model is also able to simulate the relaxation of the catalyst potential when the reaction is performed with a platinum foil in an electrochemical cell. The loss of activity as well as the relaxation of the catalyst potential can be attributed to changes in the degree of coverage by the two less reactive forms of oxygen. The latter should be considered as an extrinsic relaxation in contrast to the establishment of the steady-state degree of coverage by the reaction intermediates in the selective oxidation of ethanol, i.e., the intrinsic relaxation.

Introduction

The noble metal catalyzed oxidative dehydrogenation of aqueous alcohols or hydrated aldehydes is a reaction with many applications in carbohydrate conversion and fine chemistry. The reaction is a very clean one, using gaseous oxygen or air as the oxidant and producing only water as a side product. A recent review is given by Mallat and Baiker (1994).

Ethanol is used as a model molecule in the present paper. This reaction occurs in two stages—the oxidative dehydrogenation of ethanol

$$C_2H_5OH + {}^1/_2O_2 \rightarrow C_2H_4O + H_2O$$

followed by the oxidation of acetaldehyde

$$C_2H_4O + NaOH + {}^1/_2O_2 \rightarrow C_2H_3O_2Na + H_2O$$

From the literature (Mallat and Baiker, 1994; Vleeming et al., 1994; Schuurman et al., 1992) it appears that there are many causes of activity loss during the noble metal catalyzed oxidation of alcohols in liquid phase. One reason for activity loss is overoxidation of the catalyst surface. As the rate of overoxidation depends on the balance between the alcohol dehydrogenation during or subsequent to chemisorption and the surface oxidation of the chemisorbed species, this cause of activity loss is dominant when the reaction rate is not limited by oxygen transfer from the gas phase (Vleeming et al., 1994). Under oxygen transfer limited condition, active site coverage is at the origin of activity losses (Mallat and Baiker, 1994) and overoxidation is the result rather than the cause of the latter.

The catalyst potential during reaction is a direct indication of the oxidation state of the catalyst surface (Mallat et al., 1992; Spiro, 1986), as it is mainly influenced by the relative amounts of adsorbed species, such as adsorbed oxygen containing species and alcohol. Mallat and Baiker (1995) even suggested that through measuring the catalyst potential the rate of oxygen supply can be controlled to avoid catalyst overoxidation.

Jelemensky et al. (1995) observed that the steady-state reaction rates for ethanol oxidation in a continuous stirred-tank reactor (CSTR) are reached after a time interval, which is much higher than the so-called intrinsic relaxation time, i.e. the time corresponding to the reestablishment of a steady-state degree of coverage of the catalyst surface by the reaction intermediates (Temkin, 1976). In several experiments (Schuurman et al., 1992; Vleeming et al., 1994; Mallat and Baiker, 1994) a corresponding slow relaxation of the catalyst potential was found. As a rule, the existence of such slow relaxations is ascribed to some extrinsic phenomena rather than to pure intrinsic factors. The term extrinsic relaxation processes was introduced by Temkin (1976) and corresponds to variations in the chemical or phase composition of the surface under the effect of the reaction conditions. Extrinsic relaxation can be much slower than intrinsic relaxation. For catalytic cycles consisting of linear elementary reactions, i.e. the rate of which is proportional to the concentration of the involved intermediates, it was shown that the intrinsic relaxation time was of the order of the reciprocal of the steady-state turnover frequency.

Catalyst overoxidation also appears to result in multiple steady states (Jelemensky et al., 1995). Up to three stable steady-state rates for ethanol oxidation could be established over a feed ethanol concentration range from 300 to 400 mol m^{-3}. The upper steady state was reached by a reductive startup procedure, i.e. starting in the absence of oxygen, while the two lower steady states required an oxidative startup, i.e. starting with oxygen in the absence of ethanol. A model considering the reversible formation of less reactive oxygen adatoms and even less reactive subsurface oxygen from the reaction intermediates, OH species, which could describe the multiplicity of steady state quantitatively was developed (Jelemensky et al., 1996).

The present paper is aimed at showing that this steady-state model allows us to understand and simulate the activity loss observed during the oxidation of aqueous ethanol. The latter should be considered as an extrinsic relaxation from an initial state to a steady state. Although catalyst deactivation strictly speaking corresponds to an irreversible loss of activity, the extrinsic relaxation phenomena discussed in this work

* Author to whom correspondence should be addressed.

S0888-5885(96)00385-5 CCC: $14.00

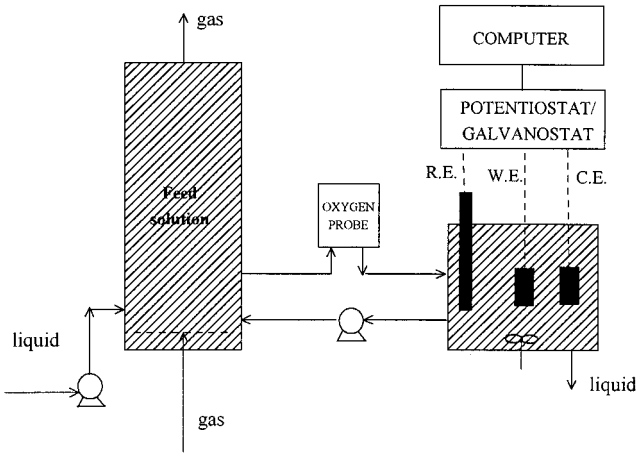

Figure 1. Continuous stirred electrochemical cell: W.E. = working electrode, R.E. = reference electrode, and C.E. = counter electrode.

have practical consequences for reactor operation very similar to those of catalyst deactivation. In analogy with catalyst deactivation the activity loss should be related as much as possible to an observable property which is a measure for its cause, e.g. coke content of the catalyst in the case of deactivation by coke deposition (Froment and Bischoff, 1990). The present paper is intended to provide more direct indications of catalyst overoxidation and its relation with steady-state multiplicity and activity loss by the measurement of the catalyst potential during reaction.

Experimental Procedures

It is in principle possible to measure the potential of the suspended catalyst powder in a CSTR. However, in order to obtain well-defined potential measurements a dedicated electrochemical cell was used in the present work.

Electrochemical Setup. The measurement of catalyst potential during the oxidation of ethanol with molecular oxygen has been carried out in a continuous flow stirred electrochemical cell with external recirculation depicted in Figure 1. Oxygen is dissolved in a separate vessel. Both the electrochemical cell and the vessel are thermostated.

Two mass flow controllers allow the feeding of different mixtures of oxygen and nitrogen to the gas inlet. A solution of ethanol was continuously fed to the vessel. The concentration of oxygen in the liquid phase is monitored by an oxygen sensor (Orbisphere 2641).

All electrochemical measurements were performed with a computer-controlled Autolab PGSTAT 20 potentiostat/galvanostat (Ecochemie). The working electrode is the catalyst of which the potential is measured under open circuit conditions. An unmodified platinum foil was used as the catalyst. No mass transport limitations occurred. As the reference electrode Hg/HgO was used. All potentials are referred to the reversible hydrogen electrode. All solutions were prepared with Millipore superQ (18 MΩ cm) water and analytical grade reagents (Merck p.a.).

The surface area of platinum metal was 4.7 cm^2, as determined from the charge associated with the anodic oxidation of the monolayer of hydrogen atoms taking place between 0 and 0.4 V. Assuming a Pt:H stoichiometry of 1:1 and a platinum number surface density of 1.31×10^{19} m^{-2}, 2.1 C m^{-2} is transferred during the oxidation of a monolayer of hydrogen atoms (Trasatti and Petrii, 1992).

For all experiments a total pressure of 101 kPa, a temperature of 298 K, a pH = 13, and a stirring speed of 20 s^{-1} was used. The ethanol feed concentration was 50 and 100 mol m^{-3}. The feed flow rate of the ethanol solution was kept constant at 3 mL/min. Under the investigation conditions the ethanol conversion was lower than 0.01%. No transport limitations occurred.

A standard pretreatment was given to the Pt electrode before a set of experiments was performed. It consisted of heating the electrode in a flame for 1 min followed by the activating procedure: 100 times the potential cycling between 0.05 and 1.6 V in 0.1 M NaOH with a scan rate of 0.1 V/s.

To study the relaxation processes of the catalyst potential from the initial state to a steady state, different start-up conditions were used. In the so-called reductive start-up procedure the potential of the working electrode was kept constant at 0.0 V for 50 s, and during the next 50 s the potential was fixed between 0.0 and 0.6 V before a step change to open circuit conditions was performed. In the so-called oxidative start-up procedure first the potential of the working electrode was kept constant at 0.0 V for 50 s and then the potential was fixed during 50 s between 0.9 and 1.5 V before a step change to open circuit conditions was performed.

It should be noted that relaxation processes were well reproducible if different initial potentials were applied before the working electrode was cycled in a minimum of 10 times between 0.5 and 1.6 V in the presence of the ethanol.

CSTR Setup. The selective oxidation of ethanol has been carried out in a continuous stirred-tank reactor containing 0.35×10^{-3} m^3 of aqueous phase and 0.347×10^{-3} kg of dry catalyst, 0.8% Pt on active carbon, at 323 K, 600 kPa total pressure, and pH = 8.4. The oxygen partial pressure in the reactor was varied between 8 and 120 kPa, and the feed ethanol concentration was between 100 and 2500 mol m^{-3}. The oxygen concentration in the liquid was set by the oxygen partial pressure being maintained in the reactor constant using a PID control for the oxygen and nitrogen feed flow rate. No transport limitations occurred.

In the reductive startup ethanol is admitted prior to oxygen; hence, the catalyst surface is occupied with dehydrogenated ethanol and is free of oxygen when the reaction starts. In the oxidative startup, ethanol is admitted after oxygen; hence, the catalyst surface is mainly occupied with oxygen-containing species when the reaction starts. A more extensive description of the experimental and start-up procedures in the CSTR setup has been given by Jelemensky et al. (1995).

It should be noted that at the start of an experiment for both start-up procedures the oxygen concentration in the liquid is not equal to the set point. It takes approximately 1500 s to reach the set oxygen concentration in the liquid. The time dependence of the oxygen concentration in the liquid was accounted for during the simulation of relaxation processes in the CSTR by an exponential relation, $P_{O_2}(t) = P_{O_2,\text{set value}} - A\, e^{(-t/B)}$, and assuming equilibrium between gas and liquid.

Model Equations

Reaction Kinetics and Mass Balances for the Surface Species. The modeling of steady-state multiplicity of the rate of selective oxidation of aqueous

ethanol over a platinum on a carbon catalyst has been reported recently by Jelemensky et al. (1996). A model which sufficiently describes the experimental data is based on the assumption that three different forms of oxygen exist on the platinum: hydroxyl, atomic oxygen, and subsurface oxygen, the former being the reaction intermediate for the ethanol oxidation. For details on the kinetics of the selective oxidation of ethanol which are described by the classical Hougen−Watson−Langmuir−Hinshelwood approach the reader is referred to Jelemensky et al. (1996). Only the features important for the relaxation will be briefly presented here.

Molecular oxygen in water irreversibly adsorbs on the surface in hydroxyl form with a rate given by

$$r_1 = k_1 C_{O_2} \theta_*^4 \, e^{(-g_{SO}\theta_{SO})} \tag{1}$$

It can be seen that the oxygen adsorption rate, r_1, strongly decreases if less free active sites are available and also decreases exponentially with an increasing degree of coverage by subsurface oxygen as was suggested by Bassett and Imbihl (1990). In contrast to the previous work (Jelemensky et al., 1996), in this work no Frumkin formalism for adsorption and desorption rate coefficients of ethanol and oxygen was assumed as the latter is not essential to describe the observations.

Thereafter adsorbed hydroxyl species slowly and reversibly are converted into atomic oxygen according to

$$r_2 = k_2 \theta_{OH}^2 \, e^{(D_O\theta_O)} \qquad r_{-2} = k_{-2} \theta_O \theta_* \, e^{(-D_O\theta_{OH})} \tag{2}$$

The rate of transformation of surface hydroxyl to surface oxygen, r_2, is strongly increased by the presence of surface oxygen, while the rate of the reverse process, r_{-2}, is decreased by the presence of surface hydroxyl species. A similar feedback is assumed for the slow reversible oxidation of the metal surface layer by formation of subsurface oxygen at a rate given by

$$r_3 = k_3 \theta_O \theta_{*SL} \, e^{(D_{SO}\theta_{SO})} \qquad r_{-3} = k_{-3} \theta_{SO} \theta_* \, e^{(-D_{SO}\theta_O)} \tag{3}$$

The reactivities of these three forms of oxygen, with respect to ethanol and aldehyde, are assumed to decrease strongly in the order of hydroxyl, atomic oxygen, and subsurface oxygen. Equations 2 and 3 introduce strong positive and negative feedback features in the model and play a key role for the description of the multiplicity of steady states. These relations cause abrupt switching between the hydroxyl species and the oxygen adatoms as dominant species on one hand and between the oxygen adatoms and subsurface oxygen on the other hand. The latter can be considered as a reconstruction of the catalyst surface. Both transformations can be interpreted as extrinsic processes.

The balances for the active sites on the surface and in the subsurface layer are given by

$$\theta_* = 1 - 2\theta_E - \theta_{OH} - \theta_{Al} - \theta_O \qquad \theta_{*_{SL}} = 1 - \theta_{SO} \tag{4}$$

where $*_{SL}$ is an empty site in the subsurface layer. Note that according to eq 4 there is no direct link between the fraction of free active sites on the surface, θ_*, and the degree of occupation of the subsurface layer by oxygen atoms, θ_{SO}.

The above considerations lead to expressions for the net production rates of the five surface species considered and allow us to simulate both the observations in the CSTR (Jelemensky et al., 1996) and in the electrochemical cell. The full model equations for the latter situation are given by the following dimensionless ordinary differential equations:

hydroxyl form

$$\frac{d\theta_{OH}}{d\tau} = \mu_O \theta_*^4 \, e^{(-g_{SO}\theta_{SO})} - 2\theta_E \theta_{OH}^2 - 2k_6' \theta_{Al} \theta_{OH}^2 - 2k_2' \theta_{OH}^2 \, e^{(D_O\theta_O)} + 2k_{-2}' \theta_O \theta_* \, e^{(-D_O\theta_{OH})} \tag{5}$$

ethanol

$$\frac{d\theta_E}{d\tau} = \mu_E \theta_*^2 - k_{-4}' \theta_E^2 - \theta_E \theta_{OH}^2 - k_8' \theta_E \theta_O - k_{10}' \theta_E \theta_{SO} \tag{6}$$

acetaldehyde

$$\frac{d\theta_{Al}}{d\tau} = \theta_E \theta_{OH}^2 + k_8' \theta_E \theta_O + k_{10}' \theta_E \theta_{SO} - k_6' \theta_{Al} \theta_{OH}^2 - k_9' \theta_{Al} \theta_O - k_{11}' \theta_{Al} \theta_{SO} - k_7' \theta_{Al} \tag{7}$$

oxygen adatoms

$$\frac{d\theta_O}{d\tau} = k_2' \theta_{OH}^2 \, e^{(D_O\theta_O)} - k_{-2}' \theta_O \theta_* \, e^{(-D_O\theta_{OH})} - k_8' \theta_E \theta_O - k_9' \theta_{AL} \theta_O - k_3' \theta_O \theta_{*SL} \, e^{(D_{SO}\theta_{SO})} + k_{-3}' \theta_{SO} \theta_* \, e^{(-D_{SO}\theta_O)} \tag{8}$$

subsurface oxygen

$$\frac{d\theta_{SO}}{d\tau} = k_3' \theta_O \theta_{*SL} \, e^{(D_{SO}\theta_{SO})} - k_{-3}' \theta_{SO} \theta_* \, e^{(-D_{SO}\theta_O)} - k_{10}' \theta_E \theta_{SO} - k_{11}' \theta_{AL} \theta_{SO} \tag{9}$$

The initial conditions for eqs 5−9 will be discussed later.

The dimensionless concentrations of oxygen and ethanol in the liquid phase are defined as

$$\mu_O = \frac{4k_1}{k_5} C_{O_2} \qquad \mu_E = \frac{k_4}{k_5} C_E \tag{10}$$

Note that only the concentrations of oxygen and ethanol and not of acetaldehyde nor of sodium acetate feature in the righthand sides of eqs 5−9 in view of the low ethanol conversion in the electrochemical cell.

Relation between Degree of Coverage by Surface Species and Catalyst Potential. The analogy between a liquid phase heterogeneous catalytic reaction and an electrochemical reaction has been treated by several authors (Mallat and Baiker, 1994, 1995; Spiro, 1986; Horanyi, 1994; Creeth and Spiro, 1991; Farchmin et al., 1993).

Some liquid phase heterogeneous catalytic reactions can be regarded as two electrochemical half-reactions proceeding on the same surface. The heterogeneous catalytic oxidation of ethanol to the corresponding aldehyde and carboxylic acid by molecular oxygen is in this way composed of

oxidation

$$CH_3CH_2OH \rightarrow CH_3CHO + 2H^+ + 2e^-$$

$$CH_3CHO + H_2O \rightarrow CH_3COOH + 2H^+ + 2e^-$$

reduction

$$O_2 + 4H^+ + 4e^- \rightarrow 2H_2O$$

The so-called mixed current−potential curve resulting from two redox couples is obtained by the addition of the two individual current−potential curves (Wagner and Traud, 1938). The steady-state potential during a chemical reaction that consists of two electrochemical half-reactions is obtained when the so-called mixed current equals zero. At potentials different from the steady-state potential the rates of the half-reactions are not in balance, resulting in a net production or consumption of electrons, which requires an external sink or source for the latter, or accumulation of charge on the catalyst. At the steady-state potential the rate of the chemical reaction is equal to the rate that corresponds to the current of the separate anodic and cathodic half-reaction.

Starting from Nernst equations no simple relation between surface coverage and the potential can be derived due to the large number of reducing and oxidizing species. Furthermore, Nernst equations correspond to thermodynamic equilibrium rather than to steady state.

Also the addition of two individual current−potential curves is only valid if the two redox couples act independently. The anodic oxidation of the alcohol may not be hindered by the presence of oxygen, and the presence of alcohol may not hinder the cathodic reduction of oxygen. There are indications in the literature (Vleeming et al., 1994; Mallat and Baiker, 1992, 1994, 1995; Schuurman et al., 1992; Gao et al., 1991; Beden et al., 1992; Chu and Gilman, 1994) that both assumptions are likely to be invalid. This means that the steady-state individual current−potential curves are not sufficient to explain the dynamic behavior of the catalyst potential during oxidation of alcohol with molecular oxygen. The suggested extension (Creeth and Spiro, 1991; Farchmin et al., 1993) of the Wagner and Traud (1938) principle, which consists of the measurement of the separate current−potential curves in the presence of the interfering redox couple, is not practical for the prediction of the behavior of the heterogeneous catalytic reaction at different conversions. This is due to the fact that current−potential curves should be recorded at a large range of concentrations of reactants and products.

In this paper it is assumed that the catalyst potential during oxidation of ethanol with molecular oxygen depends in an additive way on the degree of coverage of the different surface species. The following linear relation was assumed in first approximation between the surface composition and the catalyst potential:

$$E = E_{DL}\theta_* + E_{OH}\theta_{OH} + E_O\theta_O + E_{EA}(2\theta_E + \theta_{Al}) \quad (11)$$

The potential of the double layer E_{DL} equals 0.5 V as determined by cyclic voltammetry and corresponds to a free surface: $\theta_* = 1$. For a surface fully covered with hydroxyl the potential, E_{OH}, was taken equal to the standard potential of $Pt/Pt(OH)_2 = 0.98$ V (Nagel and Dietz, 1961; Latimer, 1952; de Bethune and Loud, 1964). For a surface fully covered with oxygen adatoms the potential, E_O, was taken equal to the standard potential of $Pt/PtO{\cdot}2H_2O = 1.04$ V (Grube, 1910). The potential of a surface fully covered with ethanol and acetaldehyde in the range of concentration of 50−100 mol m^{-3}, E_{EA}, equals 0.44 V as determined under open circuit conditions. Figure 2 shows an example of the resulting catalyst potential calculated from eq 11. Clearly, with the values of the constants in eq 11 given above, the potential gives only limited information on the state of the catalyst surface. Surfaces fully covered with either OH or O are expected to be at a potential around 1 V, whereas surfaces free of surface species or mainly covered with ethanol or acetaldehyde will have a potential around 0.5 V.

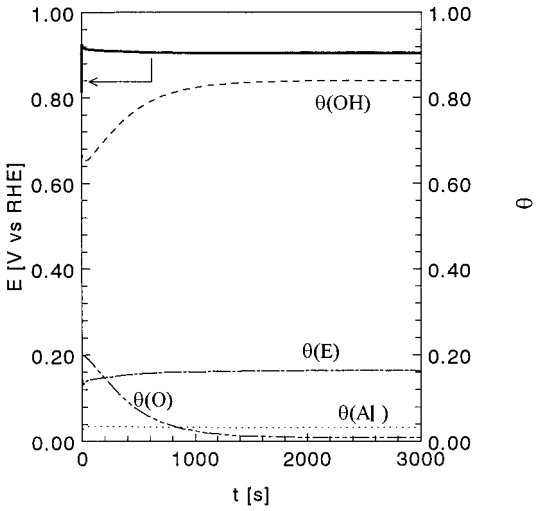

Figure 2. The platinum foil potential calculated from eqs 5−11, with parameter values in Table 1, versus time and the corresponding degree of coverage of hydroxyl, oxygen adatoms, ethanol, and acetaldehyde. Initial surface composition: $\theta_E = 0.0$, $\theta_{OH} = 0.4$, $\theta_{Al} = 0.0$, $\theta_O = 0.2$, and $\theta_{SO} = 0.0$.

In eq 11 it is assumed that the catalyst potential does not depend on the degree of coverage by subsurface oxygen. This assumption was motivated by the experimental observation that the potential increased when oxygen was adsorbed on a platinum surface in the absence of ethanol up to 1.3 V but then decreased to 1.2 V during 4000 s. Thereafter the catalyst potential slowly increased, up to 1.3 V. The model is able to explain this behavior if it is assumed that the subsurface oxygen has no direct influence on the catalyst potential. The catalyst potential increase is attributed to an accumulation of oxygen adatoms on the surface up to a sufficiently high surface concentration of oxygen adatoms to allow the formation of subsurface oxygen. At this point the oxygen adatoms are transformed into subsurface oxygen. The degree of coverage by oxygen adatoms decreases because the formation rate of subsurface oxygen, eq 3, is higher then the oxygen adsorption rate, eq 1, due to increasing degree of coverage by subsurface oxygen. This decrease in degree of coverage by oxygen adatoms results in a decrease of the catalyst potential, according to eq 11. When the second layer is sufficiently occupied by subsurface oxygen, the formation rate of subsurface oxygen decreases which results in an increase in degree of coverage by oxygen adatoms and the catalyst potential.

Experimental Results

Relaxation Processes in the Electrochemical Setup. The relaxation of the potential of the working

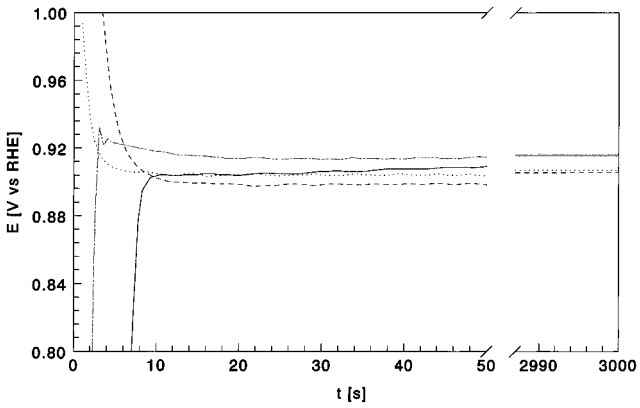

Figure 3. Platinum foil potential versus time for an ethanol concentration of 100 mol m^{-3}, $T = 298$ K, pH = 13, and an oxygen concentration of 0.84 mol m^{-3}. Potential step from (—) 0.0 V, (—·—) 0.3 V, (...) 1.3 V, (- - -) 1.5 V, to open circuit.

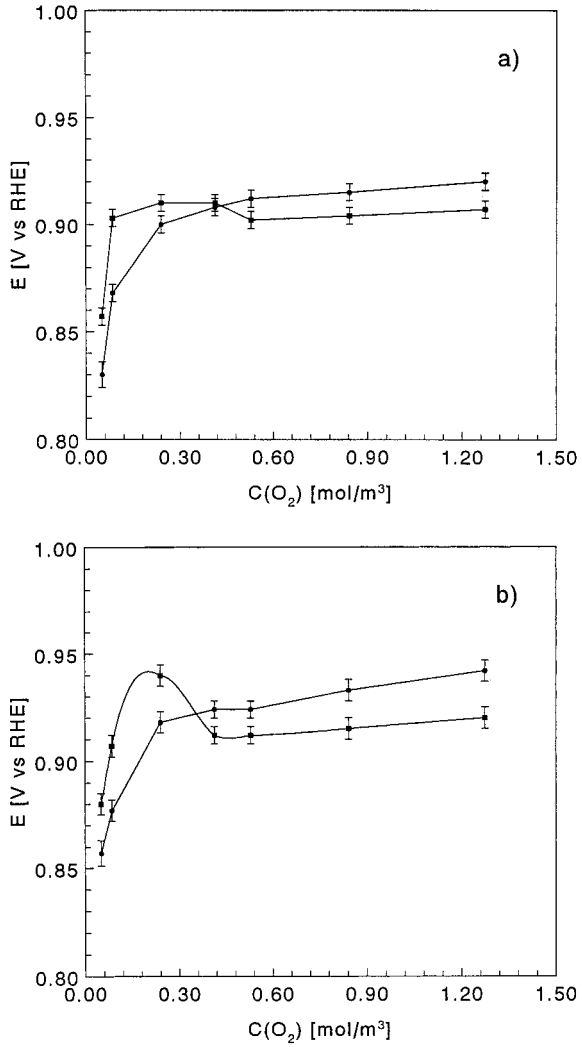

Figure 4. Steady-state platinum foil open circuit potential versus the oxygen concentration for $T = 298$ K, pH = 13, and a concentration of ethanol of (a) 100 mol m^{-3} and (b) 50 mol m^{-3}: (●) reductive startup procedure; (■) oxidative startup procedure.

electrode from different initial potentials is depicted in Figure 3. Clearly, the relaxation behavior depends strongly on the initial potential. When the potential relaxes from 0.0 V the steady-state potential is first approached within 20 s, after which it further relaxes slowly to reach the steady state after 100 s. From 0.3 V the potential relaxes through a maximum after 20 s. Then the same steady state as that starting from 0.0 V is reached after 200 s. Note that initial potentials between 0.0 and 0.4 V are thought to correspond to a reductive startup. From 1.3 V the potential reaches a steady state after 20 s. The corresponding potential is lower than the steady-state potential reached after a reductive startup. From 1.5 V the potential approaches the steady state within 50 s and then further relaxes very slowly to the same lower steady-state potential after 5000 s.

For each initial potential a distinction can be made between a fast relaxation region, which corresponds to intrinsic relaxation, and a slow relaxation toward a steady state, which corresponds to extrinsic relaxation. Furthermore, it is evident that the catalyst potential which is reached at steady state depends upon its initially imposed value, and this in a nonobvious, i.e. not intuitively expected, manner. This is why the relation between the initially imposed potential and the steady-state open circuit potential was further investigated.

Multiplicity of Steady-State Catalyst Potential in the Electrochemical Cell. Figure 4, part a, shows the steady-state potential of a platinum foil as a function of the oxygen concentration in the liquid phase for 100 mol m^{-3} of ethanol. Every experiment was repeated three to five times, and the error bars show the standard deviation from the average value. It is clear that the catalyst potential shows a multiplicity of steady states in a large range of oxygen concentrations. Furthermore, only below 0.42 mol m^{-3} of oxygen is the lower steady-state potential reached from reductive startup and the higher steady-state potential from oxidative startup as intuitively expected. Above 0.42 mol m^{-3} of oxygen, the situation is the opposite. Figure 4, part b, shows the steady-state potential as a function of the oxygen concentration in the liquid phase, but now for 50 mol m^{-3} of ethanol. Comparison of Figure 4, parts a and b, indicates that with a decrease in the ethanol concentration there is a corresponding slight decrease in the oxygen concentration which leads to a higher steady-state potential for a reductive startup than for an oxidative startup.

Relaxation Processes in the CSTR. Figure 5 shows the relaxation of the specific disappearance rates of ethanol for two startup procedures. The highest reaction rate is observed when the reductive startup was followed. For both startup procedures the relaxation consists of a monotonous decrease in the reaction rate. This decrease is more pronounced for the reductive startup.

As mentioned in the Experimental Procedures, the oxygen concentration in the liquid reaches the set value only 1500 s after a PID control for the oxygen and nitrogen feed flow rate started to control the oxygen concentration in the gas outlet. This slow establishing of the oxygen concentration obviously has an influence on the relaxation processes.

From Figure 5 it is clear that the relaxation does not correspond to intrinsic processes. The latter would, according to Temkin (1976), occur on a time scale of 4 s as the steady-state turnover frequency reached at the conditions corresponding to those of Figure 5 amounts to 0.25 s^{-1}. The steady-state reaction rate is approached after 3000 s, i.e. even much later than expected for an intrinsic process after correction for the time scale on which the oxygen liquid concentration is established.

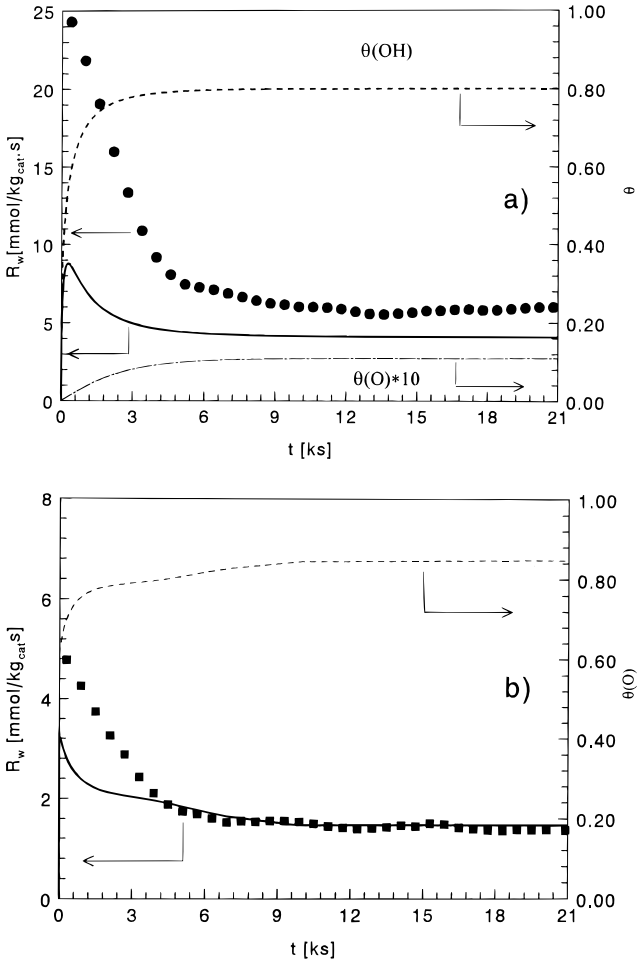

Figure 5. Specific disappearance rate of ethanol versus time for a feed concentration of ethanol of 400 mol m^{-3}, $T = 323$ K, $P_{O_2} =$ 58 kPa, pH = 8.4. (a) (●) Experimental data obtained in a CSTR with a reductive startup procedure; (full line) reaction rate calculated using equations and parameter values given by Jelemensky et al. (1996), assuming an initial surface composition given by $\theta_E = 0.5$, $\theta_{OH} = 0.0$, $\theta_{Al} = 0.0$, $\theta_O = 0.0$, and $\theta_{SO} = 0.0$ and that in the liquid phase only ethanol is present; (dashed line) degree of coverage by hydroxyl calculated in an analogous way as the reaction rate; (dashed-point line) degree of coverage by oxygen adatoms calculated in an analogous way to that of the reaction rate. (b) (■) Experimental data obtained in a CSTR with an oxidative startup procedure; (full line) reaction rate calculated using equations and parameter values given by Jelemensky et al. (1996), assuming an initial surface composition given by $\theta_E = 0.0$, $\theta_{OH} = 0.1$, $\theta_{Al} = 0.0$, $\theta_O = 0.5$, and $\theta_{SO} = 0.6$ and that in the liquid phase only ethanol is present; (dashed line) the degree of coverage by oxygen adatoms calculated in an analogous way to that of the reaction rate.

Discussion

Simulation of the Relaxation Processes in the Electrochemical Setup. The relaxation of the potential of the working electrode was simulated by eqs 5−11. The values of the kinetic parameters are given in Table 1. They are lower than those reported previously (Jelemensky et al., 1996) in order to account for the temperature difference and the difference between the catalysts used, i.e. platinum foil versus carbon-supported platinum ($d_{Pt} \approx 2$ nm). It was assumed that all the considered steps, including the feedback mechanisms involved in the transformation of the oxygen species, were activated. In particular the oxygen adsorption rate had to be lowered, reflecting the influence of Pt particle size. Furthermore it should be kept in mind that support effects will also play a role which is, up to now, not well documented.

It should be stressed that no parameter estimation by regression of the relaxation data was performed. There were two main reasons for not doing so. First, one of the purposes of this paper is to show that *steady-state* model equations sufficiently detailed to describe nonlinear phenomena, such as steady-state multiplicity, can contain the information, in particular the required rate coefficients, necessary to explain relaxation to these steady states. Second, as long as only a potential measurement characterizes the initial state of the catalyst, an element of arbitrariness is introduced. Indeed, the simulation of the relaxation requires the knowledge of the initial degrees of coverage of each of the individual species on the catalyst.

All parameters presented in Table 1 are within the range of physically realistic values (Zhdanov et al., 1988; Dumesic et al., 1993) expected. From the balances for the active sites on the surface and in the subsurface layer eq 4, it follows that the rate coefficients are correlated. It should be stressed that the model is mainly sensitive to the parameters D_O, D_{SO} and also k_2, k_{-2} and k_3, k_{-3}. For example, if $D_O < 10$ and $D_{SO} < 6$ and the rest of parameters in Table 1 are unchanged, the model predicts only one steady state. Then also relations 2 and 3 do not cause abrupt switching between hydroxyl species and oxygen adatoms and between oxygen adatoms and subsurface oxygen. On the other hand if $D_O > 10$ and $D_{SO} < 6$, the model predicts two steady states, and if $D_O > 10$ and $D_{SO} > 6$, the model predicts three steady states.

Furthermore, the time scale of the slow relaxation of the catalyst potential to the steady state strongly depends on the values of the rate coefficients k_2, k_{-2} and k_3, k_{-3}. If the model has to predict the observed time scale of the slow relaxation of the catalyst potential, the values of these rate coefficients have to be in the order 10^{-4}−10^{-5} s^{-1}. If the values are higher (10^{-2}−10^{-4} s^{-1}), then the model predicts a smaller time scale of the slow relaxation process then the one experimentally observed.

1. Initial State. In the absence of spectroscopic information there is no unambiguous relation between the startup procedures described in the Experimental Procedures and the initial degree of coverage.

The initial conditions typical for the reductive startup can be, for example, the following: only ethanol present on the surface, $\theta_E = 0.5$, corresponding to 0.44 V, the balance consisting of free surface and subsurface sites; a completely free catalyst surface and subsurface, $\theta_* = 1$ and $\theta_{*_{SL}} = 1$, corresponding to 0.5 V; a surface which is partially covered by hydroxyl and oxygen adatoms and a completely free subsurface, e.g., $\theta_E = 0.0$, $\theta_{OH} = 0.4$, $\theta_{Al} = 0.0$, $\theta_O = 0.2$, and $\theta_{SO} = 0.0$, corresponding to 0.6 V.

The initial conditions typical for the oxidative startup can be, for example, the following: a catalyst surface which is completely occupied by hydroxyl and oxygen adatoms as well as a subsurface which is partially occupied, e.g., $\theta_E = 0.0$, $\theta_{OH} = 0.7$, $\theta_{Al} = 0.0$, $\theta_O = 0.3$, and $\theta_{SO} = 0.6$, corresponding to 1 V or $\theta_E = 0.0$, $\theta_{OH} = 0.1$, $\theta_{Al} = 0.0$, $\theta_O = 0.8$, and $\theta_{SO} = 0.6$, corresponding to 0.93 V.

The fact that the model defined by eqs 5−9 considers five surface species makes it very hard to explicitly show the domains of the initial degree of coverage for each species which correspond to the reductive and oxidative

Table 1. Set of Values for the Kinetic Parameters of the Model Eqs 5−9

parameter	value	parameter	value	parameter	value
k_1^o [m^3 mol^{-1} s^{-1}]	6.2465×10^1	k_{-4}^o [s^{-1}]	2.925	k_{10} [s^{-1}]	0.001
k_2^o [s^{-1}]	3.00×10^{-5}	k_5 [s^{-1}]	1.125	k_{11} [s^{-1}]	0.001
k_{-2}^o [s^{-1}]	1.000×10^{-4}	k_6 [s^{-1}]	0.200	g_{so}	2.00
k_3^o [s^{-1}]	1.00×10^{-5}	k_7 [s^{-1}]	0.070	D_O	19.0
k_{-3}^o [s^{-1}]	1.00×10^{-5}	k_8 [s^{-1}]	0.2025	D_{so}	5.0
k_4^o [m^3 mol^{-1} s^{-1}]	0.00675	k_9 [s^{-1}]	0.0450		

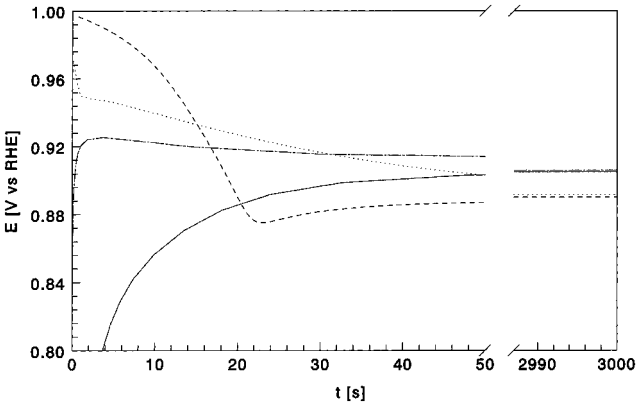

Figure 6. Catalyst potential calculated from eqs 5−11 with parameter values given in Table 1 versus time for an ethanol concentration of 100 mol m^{-3}, T = 298 K, pH = 13, and a oxygen concentration of 0.84 mol m^{-3}. Assumed initial surface composition: reductive startup, (—) $\theta_E = 0.5$, $\theta_{OH} = 0.0$, $\theta_{Al} = 0.0$, $\theta_O = 0.0$, and $\theta_{SO} = 0.0$ and (—·—) $\theta_E = 0.0$, $\theta_{OH} = 0.4$, $\theta_{Al} = 0.0$, $\theta_O = 0.2$, and $\theta_{SO} = 0.0$; oxidative startup, (- - -) $\theta_E = 0.0$, $\theta_{OH} = 0.7$, $\theta_{Al} = 0.0$, $\theta_O = 0.3$, and $\theta_{SO} = 0.6$ and (...) $\theta_E = 0.0$, $\theta_{OH} = 0.1$, $\theta_{Al} = 0.0$, $\theta_O = 0.8$, and $\theta_{SO} = 0.6$.

startup. For example, if it is assumed that in the first set of initial conditions for the oxidative startup the degree of coverage by subsurface oxygen is zero, still the same steady-state surface composition is reached. But if the initial degree of coverage by oxygen adatoms is lower than 0.22, a steady-state surface composition corresponding to a reductive startup is reached. The main difference between the reductive and the oxidative startup is that in the latter the degree of coverage by oxygen adatoms is sufficiently high.

2. Relaxation. Figure 6 shows a simulation of the relaxation of the platinum foil potential calculated from eqs 5−11 at the same conditions at which the observations reported in Figure 3 were performed. The full line corresponds to the relaxation of the system from an initial condition representative for a reductive startup, $\theta_E = 0.5$. The potential reaches the domain of the steady state after 40 s, and the steady-state potential is reached after 100 s. If the relaxation starts from another initial surface composition representative for a reductive startup, $\theta_{OH} = 0.4$ and $\theta_O = 0.2$, then the potential goes through a maximum, reaches the domain of steady state after 40 s, and then slowly relaxes to the same steady state which is reached after 100 s. It is clear that for a weakly oxidized surface, where the hydroxyl form of oxygen is dominant, the same steady-state potential is reached as from an initial surface composition where only adsorbed ethanol is present.

If the relaxation starts from a more strongly oxidized surface, then the situation is different. When the initial surface composition is $\theta_{OH} = 0.7$, $\theta_O = 0.3$, and $\theta_{SO} = 0.6$, the corresponding potential reaches the domain of the steady state after 40 s. Thereafter it very slowly relaxes toward the steady-state potential which is reached after 10 000 s. The steady-state surface composition is given by $\theta_E = 0.0394$, $\theta_{OH} = 0.0164$, $\theta_{Al} = 0.0564$, $\theta_O = 0.7244$, and $\theta_{SO} = 0.586$. The same steady state is reached from the initial surface composition $\theta_{OH} = 0.1$, $\theta_O = 0.8$, and $\theta_{SO} = 0.6$ after 100 s. It is clear that, for an oxidative startup, the time to reach the steady state strongly depends on the initial surface concentration of oxygen adatoms. If the initial degree of coverage by oxygen adatoms is far away from the steady-state degree of coverage, the relaxation to the steady state is very slow.

It is evident that the model is able to qualitatively simulate the experimental relaxation data depicted in Figure 3. The calculated potential is also characterized by a fast initial region which corresponds to intrinsic processes. On the other hand, the processes of transformation of hydroxyl into oxygen adatoms and oxygen adatoms into subsurface oxygen described by eqs 2 and 3 are a source of slow relaxation toward the steady state.

3. Steady State. Figure 7, part a, shows the calculated catalyst potential and the corresponding disappearance rate of ethanol for the conditions given in Figure 4, part a. It is clear that the model qualitatively describes the experimental steady-state data depicted in Figure 4, part a. The higher steady-state potential below 0.8 mol m^{-3} of oxygen is reached from an initial surface composition corresponding to an oxidative startup and above 0.8 mol m^{-3} from an initial surface composition corresponding to a reductive startup. The differences in steady-state potential are of course caused by differences in the coverage of the catalyst surface; see Figure 7, part b, for the degrees of coverage by OH and O. It is difficult to represent graphically the complete state of the surface, but for example, the steady-state surface composition for an oxygen concentration of 0.84 mol m^{-3} from a reductive startup corresponds to $\theta_E = 0.0085$, $\theta_{OH} = 0.8412$, $\theta_{Al} = 0.032$, $\theta_O = 0.0078$, and $\theta_{SO} = 0.00052$. This is in contrast with the situation resulting from an oxidative startup: $\theta_E = 0.0394$, $\theta_{OH} = 0.0164$, $\theta_{Al} = 0.0564$, $\theta_O = 0.7244$, and $\theta_{SO} = 0.586$. It is clear that from an oxidative startup the sum of the degree of coverage by hydroxyl and oxygen adatoms and hence, according to eq 11 the potential is lower than that from a reductive startup. As a corollary, from an oxidative startup the degree of coverage by ethanol and acetaldehyde is higher than that from a reductive startup.

According to the model, with a reductive startup, the steady-state catalyst potential increases up to 2.6 mol m^{-3} of oxygen, corresponding to a turning point, due to an increase in the degree of coverage by hydroxyl species; see Figure 7, part b. The OH species are dominant on the surface. Further increasing the liquid oxygen concentration leads to an abrupt decrease in the degree of coverage by hydroxyl, which becomes small. At this point oxygen adatoms becomes the dominant species on the surface. The corresponding steady-state catalyst potential decreases slightly up to the value which would have been obtained directly by an oxidative startup.

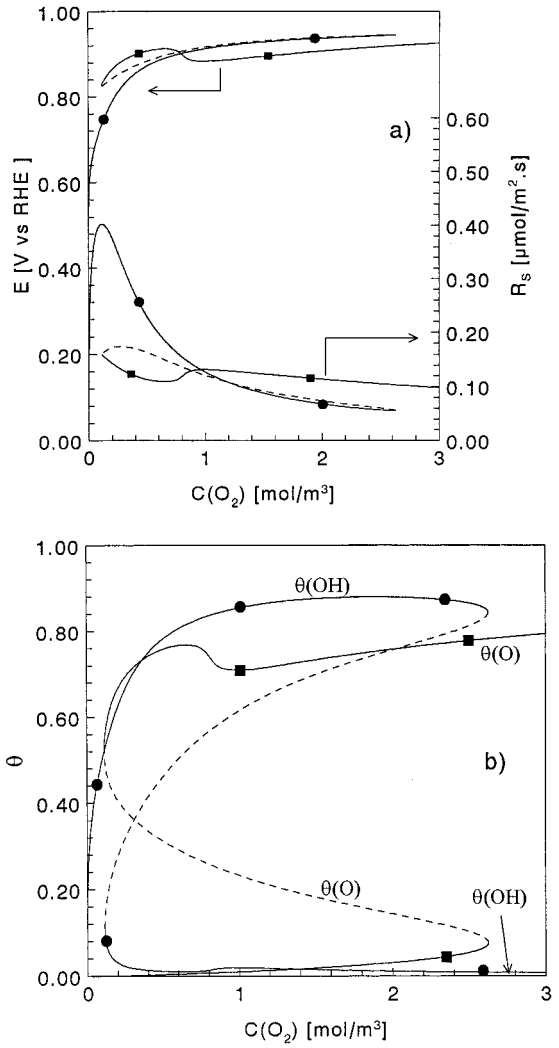

Figure 7. (a) Steady-state catalyst potential and the steady-state areal disappearance rate of ethanol in the electrochemical cell calculated from eqs 5−11 with parameter values given in Table 1 versus the oxygen concentration for $T = 298$ K, pH = 13, and an ethanol concentration of 100 mol m^{-3}. (b) Steady-state degree of coverage by a hydroxyl species and oxygen adatoms in the electrochemical cell calculated from eqs 5−11 with parameter values given in Table 1 versus the oxygen concentration for an ethanol concentration of 100 mol m^{-3}: (—) stable steady state; (- - -) unstable steady-state; calculations corresponding to (●) reductive startup procedure and (■) oxidative startup procedure.

With an oxidative startup the steady-state catalyst potential increases with increasing oxygen concentration up to 0.80 mol m^{-3} of oxygen (see Figure 7, part a) due to an increase in the degree of coverage by oxygen adatoms (see Figure 7, part b). At this point the formation rate of subsurface oxygen, eq 3, becomes higher than the oxygen adsorption rate, eq 1, due to the increasing degree of coverage by subsurface oxygen and the positive feedback of the latter on the rate of transformation of oxygen adatoms into subsurface oxygen; see Figure 7, part b. The corresponding decrease in the degree of coverage by oxygen adatoms results in an increase in the fraction of free active sites which then are partially occupied with ethanol and acetaldehyde. The corresponding catalyst potential, according to eq 11, is decreasing; see Figure 7, part a. Further increasing the oxygen concentration in the liquid phase results in an increase in the degree of coverage by subsurface oxygen up to 1 mol m^{-3}, at which point the formation rate of subsurface oxygen decreases

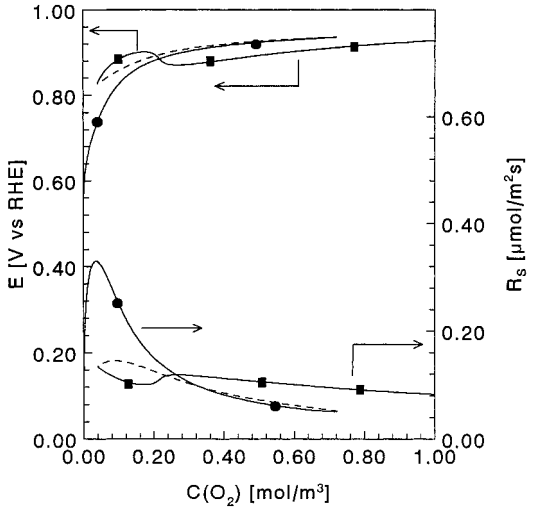

Figure 8. Steady-state catalyst potential and the steady-state areal disappearance rate of ethanol in the electrochemical cell calculated from eqs 5−11 with parameter values given in Table 1 versus the oxygen concentration for $T = 298$ K, pH = 13, and an ethanol concentration of 50 mol m^{-3}. (—) Stable steady state; (- - -) unstable steady state; calculations corresponding to (●) reductive startup procedure and (■) oxidative startup procedure.

strongly. The catalyst potential then increases again as an accumulation of oxygen adatoms on the surface now takes over.

Figure 7, part a, also shows the steady-state areal disappearance rate of ethanol. With a reductive startup the rate increases with increasing oxygen concentration as long as the degree of coverage by OH is lower than 0.50, at which point a maximum is reached. Further increasing the oxygen concentration leads to a continuous decrease of the reaction rate up to the turning point at 2.6 mol m^{-3} where an abrupt increase to the branch corresponding to an oxidative startup occurs. Note that, in the case of an oxidative startup, from 1 mol m^{-3} of oxygen the disappearance rate of ethanol is higher than that from a reductive startup. As was mentioned above, the first layer has in the former case more free active sites which can be occupied with ethanol and acetaldehyde. Such an increase in degree of coverage by ethanol and acetaldehyde results in an increase in the reaction rate. Hence, it should be stressed that a reductive startup procedure does not necessarily lead to the highest steady-state rate.

Figure 8 shows the calculated steady-state potential and the corresponding steady-state disappearance rate of ethanol for an ethanol concentration of 50 mol m^{-3} for the conditions corresponding to Figure 4, part b. In agreement with the experimental results, the model clearly indicates that with a decrease in the ethanol concentration there is a corresponding decrease in the oxygen concentration from which on a reductive startup leads to a higher steady-state potential than that on an oxidative startup. Both steady-state potential branches and, hence, their intersection shift to lower liquid oxygen concentrations.

Simulation of the Relaxation Processes in the CSTR. An example of simulation of the relaxation process of the disappearance rate of ethanol from an initial state to a steady state in the CSTR with the model and the parameter values reported by Jelemensky et al. (1996) is depicted in Figure 5 together with the observed rates. During the simulation the change of the oxygen concentration in the liquid phase in the first 1500 s was also taken into account as discussed in

the Experimental Procedures. The agreement between the calculated and observed values of the rates can be considered satisfactory as only the observed steady states were involved in the estimation of the kinetic parameters (Jelemensky et al., 1996). It is also clear that these parameter estimates do not exactly fit all transient experimental data. However, it is important to show that the calculated reaction rate relaxes to the steady state on the same time scale as the observed reaction rate. From Figure 5, part a, follows that, for an initial surface composition representative for a reductive startup, $\theta_E = 0.5$, $\theta_{OH} = 0.0$, $\theta_{Al} = 0.0$, $\theta_O = 0.0$, and $\theta_{SO} = 0.0$; in the presence of ethanol, the calculated reaction rate relaxes through a maximum, which is reached after 300 s and reaches the domain of the higher steady state after 3000 s. Thereafter the reaction rate slowly relaxes, and the higher steady state is reached after 10 000 s, corresponding with a surface composition given by $\theta_E = 0.02$, $\theta_{OH} = 0.8$, $\theta_{Al} = 0.06$, $\theta_O = 0.01$, and $\theta_{SO} = 4.0 \times 10^{-4}$.

The extrinsic relaxation of the reaction rate can be attributed to the slow increase in degree of coverage by the oxygen adatoms resulting from the transformation of hydroxyl into oxygen adatoms. From the model it follows that, if the oxidation of ethanol started from a reductive startup, the catalyst surface is weakly overoxidized by oxygen adatoms. The steady state amount of subsurface oxygen can be neglected.

Figure 5, part b, shows the simulation of the relaxation of the reaction rate from an initial surface composition representative for an oxidative startup, $\theta_E = 0.0$, $\theta_{OH} = 0.1$, $\theta_{Al} = 0.0$, $\theta_O = 0.5$, and $\theta_{SO} = 0.6$. The reaction rate also relaxes through a maximum, which is reached after 10 s. Thereafter a slow decrease in reaction rate is due to the slow formation of oxygen adatoms. The lower steady-state reaction rate is reached after 10^4 s, corresponding to a surface composition given by $\theta_E = 0.03$, $\theta_{OH} = 2.4 \times 10^{-4}$, $\theta_{Al} = 0.02$, $\theta_O = 0.85$, and $\theta_{SO} = 0.064$. With an oxidative startup the catalyst surface is more strongly overoxidized by oxygen adatoms than with a reductive startup.

Conclusions

A relative simple model with a single set of parameter values can describe at least qualitatively the existence of steady-state multiplicity and relaxation toward steady state both for the oxidation rate of ethanol and the corresponding catalyst potential. The measurement of the catalyst potential provides only limited information on the state of the catalyst, as it can at most discriminate between oxidizing and reducing species and not for instance between OH and O species. Nevertheless the measurement of the catalyst potential has allowed us to confirm the postulated reaction mechanism, in particular, the causes of the activity loss at constant conditions, which should be considered as a relaxation from an initial state to a steady state. The relaxation process is extrinsic and consists of a slow transformation of surface hydroxyl to oxygen adatoms and of the latter to subsurface oxygen.

It is believed that such transformations are at the origin of a rather broad category of so-called deactivations of noble metal catalyzed reactions, both oxidations and reductions. Also it is believed that catalyst regeneration can be described in an analogous way.

Notation

C = concentrations [m^3 s^{-1}]
D = parameter
k = reaction rate coefficient [s^{-1}] or [m^3 mol^{-1} s^{-1}]
k' = dimensionless reaction rate coefficient in eqs 5−9 defined as $k' = k_i/k_5$
P_{O_2} = oxygen partial pressure [Pa]
R_w = disappearance rate [mol kg_{cat}^{-1} s^{-1}]
R_S = disappearance rate [mol m^{-2} s^{-1}]
t = time [s]
W = mass of dry catalyst [kg]

Greek Symbols

θ = fraction of total number of active sites
σ = stoichiometric number
τ = dimensionless time defined as $\tau = tk_5$

Subscripts

1, 2, 3 ... = number of reaction step
E = ethanol
Al = acetaldehyde
Ac = sodium acetate
* = free active surface site
O = atomic oxygen
SO = subsurface oxygen
SL = subsurface layer
DL = double layer

Superscripts

o = for $\theta^* = 1$

Literature Cited

Bassett, M. R.; Imbihl, R. Mathematical Modelling of Kinetic Oscillations in the Catalytic CO Oxidation on Pd(110): The Subsurface Oxygen Model. *J. Chem. Phys.* **1990**, *93*, 811.

Beden, B.; Léger, J.-M.; Lamy, C. Electrocatalytic Oxidation of Oxygenated Aliphatic Organic Compounds at Noble Metal Electrodes. In *Modern Aspects of Electrochemistry*; Bockris, J. O'. M., et al., Eds.; Plenum Press: New York, 1992; Vol. 22, p 97.

Chu, D.; Gilman, S. The Influence of Methanol on O_2 Electroreduction at a Rotating Pt Disk Electrode in Acid Electrolyte. *J. Electrochem. Soc.* **1994**, *141*, 1770.

Creeth, A. M., Spiro, M. A Re-Formulation of the Wagner and Traud Additivity Principle: Catalytic and Electrochemical Experiments with Iodide Modified Surfaces. *J. Electroanal. Chem.* **1991**, *312*, 165.

Dumesic, J. A.; Rudd, D. F.; Aparicio, L. M.; Rekoske, J. E.; Treviño, A. A. *The Microkinetics of Heterogeneous Catalyst*; ACS Professional Reference Book; American Chemical Society: Washington, DC, 1993.

de Bethune, A. J.; Loud, N. A. S. *Standard Aqueous Electrode Potentials and Temperature Coefficients*; Clifford A. Hampel: Skokie, IL, 1964.

Farchmin, R. O.; Nickel, U.; Spiro, M. Heterogeneous Catalysis in Solution. Part 26. *J. Chem. Soc., Faraday Trans.* **1993**, *89*, 229.

Froment, G. F.; Bischoff, K. B. *Chemical Reactor Analysis and Design*, 2nd ed.; Wiley Series in Chemical Engineering; Wiley: New York, 1990; Chapter 5, p 219.

Gao, P.; Lin, G. H.; Shannon, C. H.; Salaita, G. N., White, J. H.; Chaffins, S. A.; Hubbard, A. T. Studies of Adsorbed Saturated Alcohols at Pt(111) Electrodes by Vibrational Spectroscopy (EELS), Augar Spectroscopy and Electrochemistry. *Langmuir* **1991**, *7*, 1515.

Grube, G. *Z. Elektrochem.* **1910**, *16*, 62.

Hoare, J. P. *The Electrochemistry of oxygen*; Interscience Publishers: New York, 1968.

Horanyi, G. Heterogeneous Catalysis and Electrocatalysis. *Catal. Today* **1994**, *19*, 285.

Jelemensky, L.; Kuster, B. F. M.; Marin, G. B. Multiple Steady-States for the Oxidation of Aqueous Ethanol with Oxygen on a Carbon Supported Platinum Catalyst. *Catal. Lett.* **1995**, *30*, 269.

Jelemensky, L.; Kuster, B. F. M.; Marin, G. B. Kinetic Modelling of Multiple Steady-States for the Oxidation of Aqueous Ethanol with Oxygen on a Carbon Supported Platinum Catalyst. *Chem. Eng. Sci.* **1996**, *51*, 1767.

Latimer, W. M. *Oxidation Potentials*, 2nd ed.; Prentice Hall: Englewood Cliffs, NJ, 1952.

Mallat, T.; Baiker, A. Oxidation of Alcohols with Molecular Oxygen on Platinum Metal Catalysts in Aqueous Solution *Catal. Today* **1994**, *19*, 247.

Mallat, T.; Baiker, A. Catalyst Potential: a Key for Controlling Alcohol Oxidation Reactors. *Catal. Today* **1995**, *24*, 143.

Mallat, T.; Baiker, A.; Botz, L. Liquid Phase Oxidation of 1-Methoxy-2-Propanol with Air-III. Chemical Deactivation and Oxygen Poisoning of Platinum Catalyst. *Appl. Catal., A* **1992**, *86*, 147.

Nagel, K.; Dietz, H. Spannungs-Aktivitäts-Diagramm der Wichtigsten Elektrodenreaktionen im System Platin/Platinoxid/Lösung. *Electrochim. Acta* **1961**, *4*, 141.

Schuurman, Y.; Kuster, B. F. M.; van der Wiele, K.; Marin, G. B. Selective Oxidation of Methyl α-D-Glucoside on Carbon Supported Platinum − III. Catalyst Deactivation. *Appl. Catal., A: General* **1992**, *89*, 47.

Spiro, M. Polyelectrodes: The Behaviour and Applications of Mixed Redox Systems. *Chem. Soc. Rev.* **1986**, *15*, 141.

Temkin, M. I. The Kinetics of Steady-State Complex Reactions. *Kinet. Katal.* **1976**, *17*, 1095.

Trasatti, S.; Petrii, O. A. Real Surface Area Measurements in Electrochemistry. *J. Electroanal. Chem.* **1992**, *327*, 353.

Vleeming, J. H.; de Bruijn, F. A.; Kuster, B. F. M.; Marin, G. B. Deactivation of Carbon-Supported Platinum Catalyst During Oxidation in Aqueous Media. In *Catalyst Deactivation*, Delmon B., Froment G. F., Eds.; Studies in Surface Science and Catalysis, **1994**, *88*, 467.

Zhdanov, V. P.; Pavliček, P.; Knor, Z. Preexponential Factors for Elementary Surface Processes. *Catal. Rev.-Sci. Eng.* **1988**, *30*, 510−517.

Wagner, C.; Traud, W. Über die Deutung von Korrosionsvorgängen Durch Überlagerung von Elektrochemischen Teilvorgängen und Über die Potentialbildung an Mischelektroden. *Z. Elektrochem.* **1938**, *44*, 391.

Received for review July 8, 1996
Revised manuscript received December 11, 1996
Accepted February 11, 1997[⊗]

IE960385N

[⊗] Abstract published in *Advance ACS Abstracts,* June 15, 1997.